Size controlled and optical properties of Zn- doped SnO_2 nanoparticles via sol-gel process

J. GAJENDIRAN*, V. RAJENDRAN
Department of Physics, Presidency College, Chennai-600 005, Tamilnadu, India

Zn- doped SnO_2 nanocrystallites were prepared by taking $SnCl_4.5H_2O$ as precursor, using water as a solvent via sol-gel process. X-ray diffraction (XRD), Fourier transform infrared spectra (FTIR),Thermal gravimmetry spectrometry (TGA),Scanning electron microscopy (SEM),Transmission electron microscopy (TEM), Energy Dispersive X-ray analysis (EDX), UV-Vis spectroscopy and Photoluminescence (PL) were used to analyzed the crystal structure, particle size, molecular structures and optical properties of the prepared SnO_2 nanoparticles. The XRD pattern revealed that the tetragonal rutile phase and the average crystallites size were calculated to be 10 nm for Zn-doped SnO_2 nanoparticles calcined at 600ºC. The spherical-like morphology of the as-synthesized Zn-doped SnO_2 nanoparticles was observed in the SEM and TEM studies. Zn-doped SnO_2 nanoparticles were exhibit enhanced UV emission at ~ 394 nm and could be used as nanoscale optoelectronic devices

(Received July 7, 2010; accepted January 26, 2011)

Keywords: Semiconductor, Nanoparticles, SnO_2, Sol-gel, Optical properties

1. Introduction

As a transparent semiconductor (Eg=3.6eV at 300 K [1]), SnO_2 is of great scientific and technical interest in view of its versatile applications in transparent conductive electrode, gas sensors, and photovoltaic devices, etc. It is generally accepted that the practical performances of SnO_2 are relative to its crystallinity, morphology, crystal size, crystal defects, and surface properties, etc, which ultimately depend on the preparation methods and preparation conditions [1-9]. SnO_2 nanopowders are semiconducting inorganic nanocrystallites with dimensions less than 100 nm, in all three dimensions. Consequently, discrete electronic states, unusual structural transformations, unique optical properties and a blue shift of the band edge transitions energy are induced in these nanoparticles [10-13]. Due to high surface-to-volume ratio, the surface atoms play a large role in the properties of nanomaterials, which usually have fewer adjacent coordinated atoms and can be treated as defects as compared with the bulk atoms. These defects induce additional electronic states in the band gap, which can mixed with the intrinsic states to a substantial extent and which may influence the spacing of the energy levels and the optical properties of nanopowders. Various methods have been used to prepare SnO_2 nanostructures, such as hydrothermal method [14, 15], polymeric [16] and organometallic precursor synthesis [17], soncation procedure [18, 19], microwave synthesis [20, 21] and surfactant-mediated method [22]. In spite of the fact that all the above mentioned method towards controlling SnO_2 particle size have been proven to be impressive and effective, however, some drawbacks are also present with these methods. For instance, time-consuming is a big concern for these methods. It takes at least 24h for the hydrothermal method [14, 15] to obtain the final SnO_2 nanoparticles products. Besides, the complicated processes of the polymeric precursor [16] synthesis and sonication procedure [18, 19] are also not favorable for practical applications considering large-scale synthesis, fabrication cost and facile preparation process. Sol-gel, processing is a relatively simple way of preparing chemically homogeneous, high purity and phase-pure powders at a lower temperature. However, some major drawbacks present in the extensively applied sol-gel procedures based on the hydrolysis and condensation of metal-halide or alkoxide precursors in aqueous solution remain. In the most cases, the as synthesized precipitates are amorphous and heat treatment is necessary to induce crystallization resulting either in alteration, mainly particle growth, or even in changing the particle morphology. Synthesis of SnO_2 nanomaterials doped with metal ions, such as Sc [23], Pd [24] and Ni-doped [25] has been reported.

In this paper, Zn-doped SnO_2 nanocrystalline were synthesized using the sol-gel process. The as-synthesized spherical like Zn-doped SnO_2 nanoparticles were found to exhibit enhanced UV emission peak at 394nm and could be used as nanoscale optoelectronic devices.

2. Experimental

All chemicals were analytical grade (AR) purity and used without further purification. In a typical synthesis, $SnCl_4$ solutions were made by dissolving $SnCl_4.5H_2O$ (6.9 g) in 100 ml distilled water. Then, hydrochloric acid (2 ml) was added to prevent the rapid hydrolysis of $SnCl_4$. The aqueous ammonia solution (3.7 ml) was added drop wise into one flask containing the $SnCl_4$ solution (30 ml) under vigorous stirring at room temperature to adjust the pH of

the solution about1. The resultant white sol was heated at 60ºC for 30 min under vigorous stirring. Subsequently, $ZnCl_2$ (0.0681g) was added slowly, and the mixture was stirred for 2h at 60 ºC.After aging for two days, the sol was filtered washed with distilled water to remove the chlorine ions from the system. Then, the product was dried in a vacuum at 50 ºC for 4h. Finally, sample were annealed at four different temperatures in the muffle furnace (150, 300, 450 and 600 ºC for 2h) for producing Zn-doped SnO_2 nanoparticles.

The obtained samples were characterized by X-ray powder diffraction (XRD). XRD pattern was collected on a schimadzu model; XRD 6000 with CuKα radiation (λ= 1.5417 Å), at scanning rate of 0.04s-1 was applied to record the pattern in the range 20–70º. The chemical structure information of the particles was collected by FT-IR spectra (Nicolet 205 spectrometer). Scanning electron microscope (SEM) analysis was carried out for the sample on a JEOL- JEM - 3010 SEM using an accelerating voltage of 10 kV. Transmission electron microscope (TEM) and Energy dispersive X-ray spectrum analysis (EDS) were carried out for the sample on a Philips model CM-20 TEM. UV-Vis absorption spectra of the samples were recorded at room temperature by using Varian cary5E spectrophotometer. The photoluminescence (PL) spectra of the SnO_2 were recorded by Perkin-Elmer lambda 900 spectrophotometer with a Xe lamp as the excitation light source. Thermo gravimetric analysis (TGA) was performed using a model Hi.Res.2950 instrument in the temperature range of 50-850ºC in nitrogen atmosphere.

3. Result and discussion

The XRD patterns of the as synthesized Zn-doped SnO_2 nanopowders at different annealing temperatures are shown in Fig. 1 (a-d). It is clear that powders that are amorphous (Fig. 1a) and these annealed at 300 ºC (Fig. 1b) are slightly crystallized with amorphous background. Those annealed at 450 ºC are well-improved crystalline nature (Fig. 1c). Finally, those samples annealed at 600 ºC (Fig. 1d) are well crystallized. Certainly, crystallization starts at 300 ºC and amorphous background falls down. Braggs peaks of the crystallized powders correspond to each sample agree well with the reflections of tetragonal rutile Also, with good agreement of tetragonal rutile phase SnO_2 (JCPDS file No.41-1445). The average crystallites sizes calcined at 600 ºC of the Zn-doped SnO_2 nanoparticles were calculated to be 10 nm by using Scherrer's formula.

Fig. 2 shows the FTIR spectra of the prepared Zn-doped SnO_2 samples at 300 ºC and after calcining at 450ºC. As to the sample at 300 ºC, an intense, very broad IR peak ranging from 3700 to 1400 cm^{-1}, with two maximum at 1625 and 1401 cm^{-1}, which may be due to –OH and NH_3 vibration. After calcinations at 450 ºC, the peak at 1625 cm^{-1} becomes much weaker. The band centered at 1401 cm^{-1} may also related to NH_3. Increasing calcining temperature results in the decrease of the intensity of the water band, and after heating at 450 ºC, the bands attributed NH_3 around at 1401 very weak peak. Two intense broad bands at 664 and 529 cm^{-1} of the sample at 300 ºC are observed. After calcining at 450 ºC, the intensity of these two bands increases remarkably. These bands are assigned to the antisymmetric Sn-O-Sn stretching mode of the surface- bridging oxide formed attributed to changes in the size and shape of the SnO_2 particles by condensation of adjacent surface hydroxyl groups.

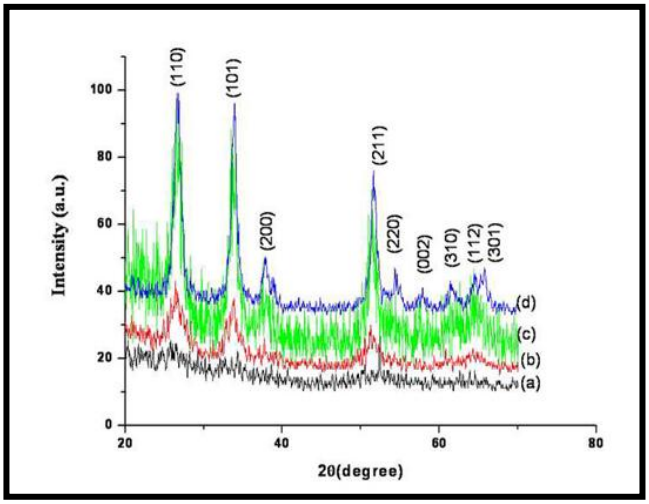

Fig. 1. XRD pattern of as-synthesized Zn-doped SnO_2 nanoparticles heat - treated at (a) 150 ºC, (b) 300 ºC, (c) 450 ºC, (d) 600 ºC.

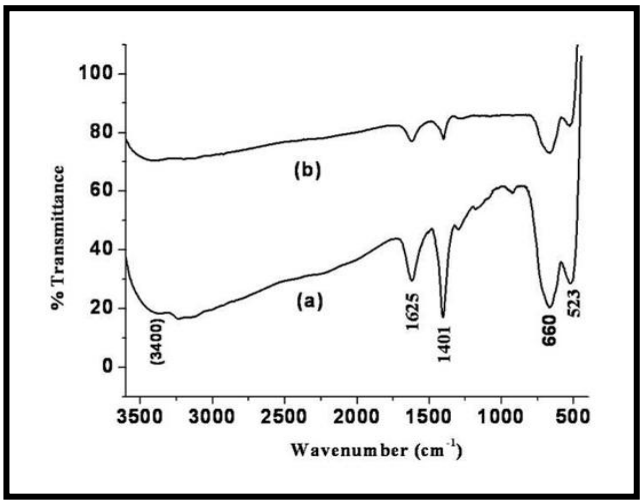

Fig. 2. FTIR spectra of as-synthesized Zn-doped SnO_2 nanoparticles heat-treated at (a)300 ºC, (b) 450 ºC.

Fig. 3 shows the SEM micrographs of Zn-doped SnO_2 nanoparticles prepared at different calcinations temperatures. As shown in Fig. 3a, the as-synthesized

samples consist of fine tiny spherical nanoparticles were observed in the calcined at 300 ºC. However, in the case of 600 ºC Zn-doped SnO_2 nanoparticles (Fig. 3b) revealed to be well-crystallized and also slightly agglomerated spherical nanoparticles in the size range of ~10 nm. Due to the high grain growth and increased in particle size was observed from the samples calcined at 600 ºC than that of the calcined at 300 ºC as shown in Fig. 3a.

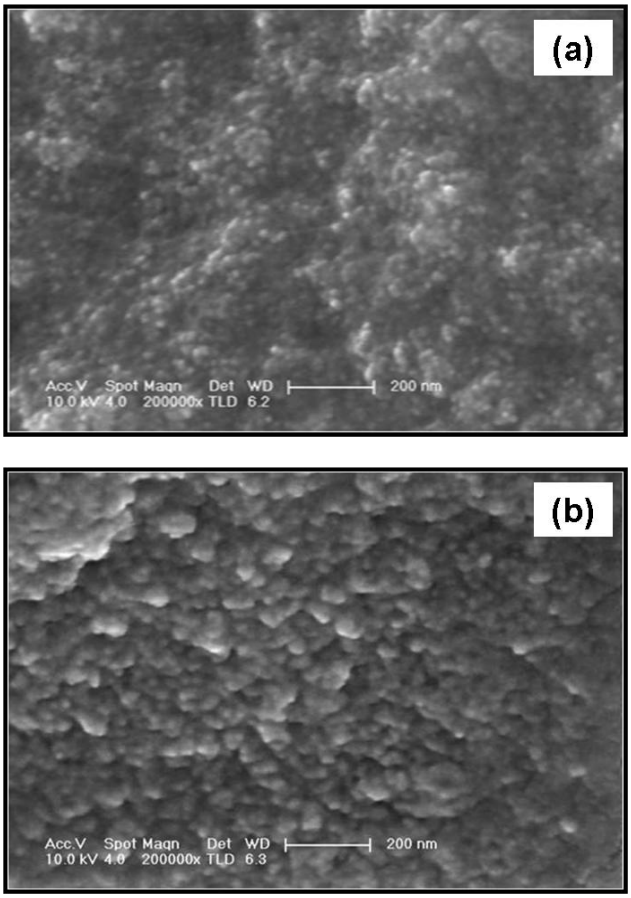

Fig. 3. SEM images of as-synthesized Zn-doped SnO_2 nanoparticles heat-treated at (a) 300 ºC, (b) 600 ºC.

Fig. 4 show the TEM images of the Zn-doped SnO_2 nanoparticles obtained by sol-gel method calcined at (a) 300 ºC and (b) 600 ºC. In the figures, particle sizes of SnO_2 heated at respective temperatures show good agreement with the result of SEM images shown in Fig. 3a and 3b.

Fig. 5 shows that the EDX pattern of the Zn doped SnO_2 nanoparticles at 300 ºC. Signs of elements O, Sn, Cu and Zn are observed in the pattern, among which Cu came from the TEM grid respectively. Therefore, the sample was composed of 62.20%-O, 36.30%-Sn and 1.50%-Zn, which clearly indicates that the synthesized sample is Zn doped tin oxide nanoparticles.

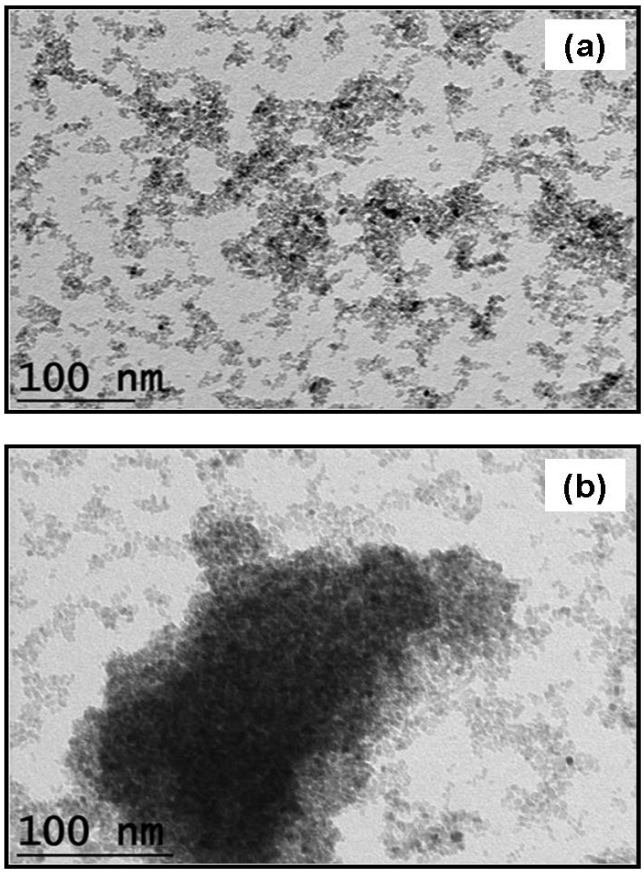

Fig. 4. TEM images of as-synthesized Zn-doped SnO_2 nanoparticles heat-treated at (a) 300 ºC, (b) 600 ºC.

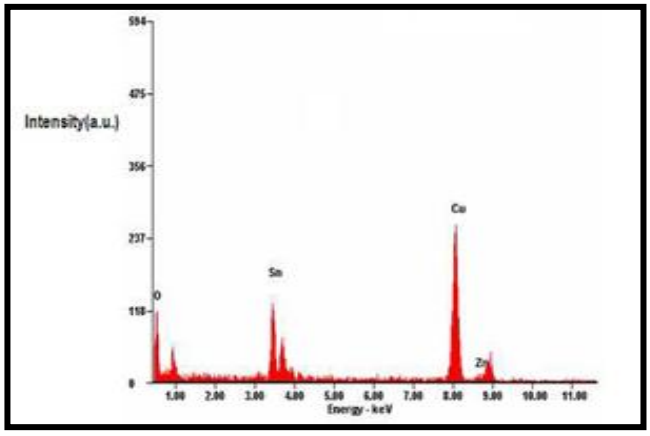

Fig. 5. EDX spectrum of as-synthesized Zn-doped SnO_2 nanoparticles heat-treated at 300 ºC.

Nanosized semiconductor particles generally exhibits a threshold energy in the optical absorption measurements, due to the size –specific band gap structures [26-28],which is reflected by the blue shift of the absorption edge with decreasing particles size. The optical absorption spectra of the samples calcined at different temperatures (300 and 600 ºC, respectively) are shown in Fig. 6. Considering the blue shift of the absorption positions from the bulk SnO_2, the absorption onsets of the presents samples can be

assigned to the direct transition of electron in the SnO_2 nanocrystals. The band gap is found to be particle size dependent and increases with decreasing particle size. The absorption onset of the sample (a) and sample (b) are 315 and 322 nm. Fig. 6 the corresponding band gap energy can be calculated to be 3.93 and 3.85 eV and is large than the value of bulk SnO_2 (3.6 eV) [29].

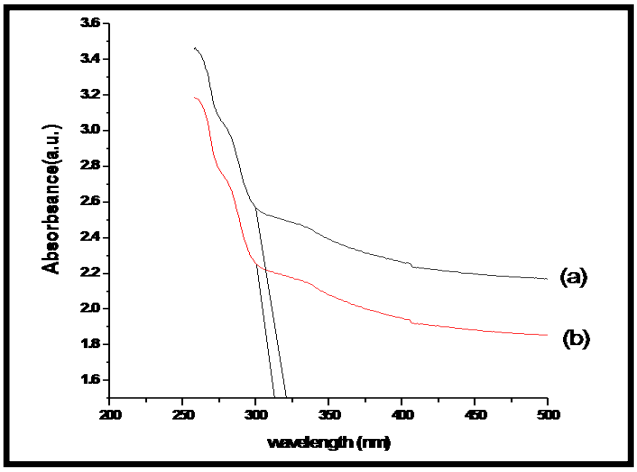

Fig. 6. UV absorption spectra of as-synthesized Zn-doped SnO_2 nanoparticles heat treated at (a) 300 ºC, (b) 600 ºC.

The emission spectra of the as-synthesized Zn-doped SnO_2 nanoparticles are shown in Fig. 7a & 7b. A strong UV emission peak at ~394 nm and several weak emission peaks are observed in the visible region in both cases. The emission in the UV region is due to recombination of excitonic centers and corresponds to the near band edge emission. The emission in the visible region is due to defects in SnO_2 such as vacancies and interstitials. The weak intensity of the emission peaks in the visible region indicated that the defects are in low concentration and SnO_2 nanocrystals are of good quality in both cases.

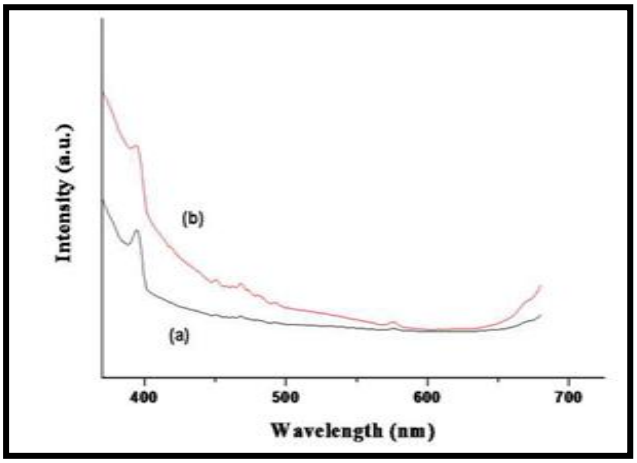

Fig. 7. PL emission spectra of as-synthesized Zn-doped SnO_2 nanoparticles heat – treated at (a) 300 ºC, (b) 600 ºC.

Fig. 8 shows the rate of weight loss of the particles as a function of temperature by thermogravimetric analysis (TGA). The rate of weight loss (5.5%) was observed between 50 and 150 ºC, which can come from the evaporation of physically absorbed water and NH_3 in the particles. The second weight loss (38%) was observed between 150 and 450 ºC, which can come from the organics residues in the particles. The third weight loss (9.2%) may come from the decomposition of Sn $(OH)_4$. Above 600 ºC no weight loss is observed in the TGA curve. This result is quite similar to results obtained from XRD analysis as shown in Fig. 1d.

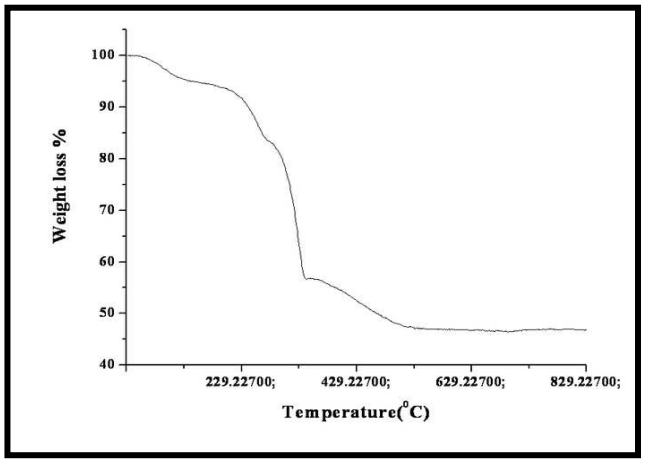

Fig. 8. TGA curve of as-synthesized Zn-doped SnO_2 nanoparticles heat-treated at 150 ºC.

4. Conclusion

In summary, Zn-doped SnO_2 nanocrystallites were synthesized successfully by sol –gel method using water as a solvent. The XRD pattern revealed that the tetragonal rutile phase and the average crystallites size were calculated to be 10 nm for Zn-doped SnO_2 nanoparticles calcined at 600 ºC. The absorption band edges were observed that 315 and 322 nm the corresponding band gap energy can be calculated to be 3.93 and 3.85 eV is larger than the value of bulk SnO_2 (3.6eV). Zn-doped SnO_2 nanoparticles were exhibit enhanced UV emission at 394 nm and could be used as nanoscale optoelectronic devices. Weak intensity of the emissions in the visible region indicates that the defects are in low concentration and SnO_2 nanocrystals are of good quality with little surface defects in both cases. The spherical like morphologies of as-synthesized Zn-doped SnO_2 nanoparticles were observed in the SEM and TEM studies. Usually heat post-treatment at high temperature is necessary for removal of organic residues and to acquire perfect nanocrystalline SnO_2. In addition, this sol-gel method is more economic, time- saving, human and environment friendly, as it requires no use of toxic organic solvents, surfactant or special laboratory apparatus such as microwave and sonication.

Acknowledgment

The authors are grateful to the Tamilnadu state Council for Science and Technology, for extending financial assistance to carry out this work.

References

[1] J. Q. Sun, J. S. Wang, X. C. Wu, Cryst. Growth Des, **6**, 1584 (2006).
[2] J. Duan, S. Yang, H. Liu, J. Am. Chem. Soc. **127**, 6180 (2005).
[3] X. M. Han, B. Zhang, S. K. Guan, J. Alloy Compd. **461**, L26 (2008).
[4] T. Gao, T. H. Wang, Mater. Res. Bull, **43**, 836 (2008).
[5] S. H. Sun, G. W. Meng, G. X. Zhang, Chem. Phys. Lett, **376**, 103 (2003).
[6] H. W. Kim, S. H. Shim, C. Lee, Ceram. Int. **32**, 943 (2006).
[7] D. Cai, Y. Su, Y. Q. Chen, Mater. Lett. **59**, 1984 (2005).
[8] J. Q. Hu, Y. Bando, D. Golberg, Chem. Phys. Lett. **372**, 758 (2003).
[9] Z. Y. Huang, C. F. Chai, Mater. Lett. **61**, 5113 (2007).
[10] M. Law, H. Kind, B. Messer, F. Kim, P. D. Yang, Angew, Chem; Int. Ed. Engl, **41**, 2405 (2002).
[11] Y. Wang, X. Jiang, Y. Xia, J. Am. Chem. Soc. **125**, 16176 (2003).
[12] Y. S. He, J. C. Campbell, R. C. Murphy, M. F. Arendt, J. S. Swinnea, J. Mater. Res. **8**, 3131 (1993).
[13] P. G. Harrison, M. J. Willet, Nature. **332**, 337 (1988).
[14] H. C. Chiu, C. S. Yeh, J. Phys. Chem. **C111**, 7256 (2007).
[15] A. A. Firooz, A. R. Mahjoub, A. A. Khodadadi, Mater. letter, **62**, 1789 (2008).
[16] E. R. Leite, I. T. Weber, E. Longo, J. A. Varela, Adv. Mater. **12**, 965 (2000).
[17] C. Nayral, E. Viala, P. Fau, F. Senocq, J. C. Jumas, A. Maisonnat, B. Chaudret, Chem. Eur. J. **6**, 4082 (2000).
[18] J. Zhu, Z. Lu, S. T. Aruna, D. Aurbach, A. Gedanken, Chem. Mater. **2**, 2557 (2000).
[19] G. Pang, S. Chen, Y. Koltypin, A. Zaban, S. Feng, A. Gedanken, Nano Lett **1**, 723 (2001).
[20] V. Subramanian, W. W. Burke, H. Zhu, B. Wei, J. Phys. Chem. **C112**, 4550 (2008).
[21] J. Jouhannaud, J. Rossignol, D. Stuerga, J. Solid State Chem. **181**, 1439 (2008).
[22] Y. D. Wang, C. L. Ma, X. D. Sun, H. D. Li, Nanotechnology **13**, 565 (2002).
[23] G. Xu, Y. W. Zhang, X. Sun, C. L. Xu, C. H. Yan, J. Phys. Chem. **B109**, 3269 (2005).
[24] S. C. Tsang, C. D. A Bulpitt, P. C. H. Mitchell, A. J. Ramirez-Cuesta, J. Phys. Chem, **B105**, 5737 (2001).
[25] P. Hidalgo, R. H. R Castro, A. C. V. Coelho, D. Gouvea, Chem. Mater. **17**, 4149 (2005).
[26] A. Henglein, Chem. Rev. **89**, 1861 (1989).
[27] Y. Wang, N. Herron, J. Phys. Chem, **95**, 525 (1991).
[28] H. Weller, Adv. Mater. **5**, 88 (1993).
[29] A. Aoki, H. Sarakura, Jpn, J. Appl. Phys. **9**, 582 (1970).

*Corresponding author: gaja_1986msc@yahoo.co.in